



**Abstract**—In the Gulf of Mexico, the red drum (*Sciaenops ocellatus*) is an immensely popular sportfish, yet the Gulf of Mexico stock is currently managed as data-limited in federal waters. The results of the federal stock assessment conducted in 2016 for Gulf of Mexico red drum were not recommended for providing management advice. Consequently, we sought to address data gaps highlighted in the assessment by producing up-to-date overall and sex-specific growth models, standardized indices of relative abundance, and predictions of habitat suitability and by updating estimates of natural mortality. Using a time series for the period of 2006–2018, we assigned ages of 0–36 years to 1178 red drum. A negative binomial generalized linear model including variables for year, depth, surface temperature, dissolved oxygen, and bottom salinity was used to standardize an index of relative abundance. Examination of catch per unit of effort revealed that adult red drum were significantly more abundant in state waters than in federal waters. These findings were explained by habitat suitability models, which were used to identify surface current velocity, surface temperature, and depth as the strongest predictors of relative abundance. The results of our investigation reveal that the adult spawning stock of red drum in the Gulf of Mexico is not fully protected by the catch moratorium in federal waters.

## Population dynamics, relative abundance, and habitat suitability for adult red drum (*Sciaenops ocellatus*) in nearshore waters of the north-central Gulf of Mexico

**Crystal L. Hightower**<sup>1,2</sup>  
**J. Marcus Drymon**<sup>3,4</sup>  
**Amanda E. Jefferson**<sup>3,4</sup>  
**Matthew B. Jargowsky**<sup>3,4</sup>

**Emily A. Seubert**<sup>3</sup>  
**Simon Dedman**<sup>5</sup>  
**John F. Mareska**<sup>6</sup>  
**Sean P. Powers (contact author)**<sup>1,2</sup>

Email address for contact author: [spowers@disl.edu](mailto:spowers@disl.edu)

<sup>1</sup> Department of Marine Sciences  
University of South Alabama  
5871 USA Drive North  
Mobile, Alabama 36688

<sup>2</sup> Dauphin Island Sea Lab  
101 Bienville Boulevard  
Dauphin Island, Alabama 36528

<sup>3</sup> Coastal Research and Extension  
Center  
Mississippi State University  
1815 Popp's Ferry Road  
Biloxi, Mississippi 39532

<sup>4</sup> Mississippi-Alabama Sea Grant Consortium  
703 East Beach Drive  
Ocean Springs, Mississippi 39564

<sup>5</sup> Hopkins Marine Station  
Stanford University  
120 Oceanview Boulevard  
Pacific Grove, California 93950

<sup>6</sup> Marine Resources Division  
Alabama Department of Conservation and  
Natural Resources  
PO Box 189  
Dauphin Island, Alabama 36528

Manuscript submitted 1 November 2021.  
Manuscript accepted 9 May 2022.  
Fish. Bull. 120:162–175 (2022).  
Online publication date: 19 May 2022.  
doi: [10.7755/FB.120.2.6](https://doi.org/10.7755/FB.120.2.6)

The views and opinions expressed or implied in this article are those of the author (or authors) and do not necessarily reflect the position of the National Marine Fisheries Service, NOAA.

Advances in approaches to data collection and statistical techniques have ushered in the next generation of stock assessments (Lynch et al., 2018). For data-rich species, stock assessments can incorporate ecosystem-based inputs (Lynch et al., 2018), often through the use of spatially explicit approaches (e.g., Goethel et al., 2011; Berger et al., 2017). Despite these advances, more than half of U.S. stocks remain data-limited (Newman et al., 2015). Enhancing basic data inputs is imperative for improving assessments for these stocks. For stocks under aggressive rebuilding schedules, those for which catch data may not reflect population trends or for which catch is completely restricted, the need for reliable time series that track abundance is even more critical.

In the Gulf of Mexico (GOM), the red drum (*Sciaenops ocellatus*) is a highly prized species supporting valuable recreational fisheries. Recreational catch of red drum is permitted in all state waters in the GOM (out to 3 nautical miles [nmi] in Louisiana, Mississippi, and Alabama and out to 9 nmi in Texas and Florida), but a catch moratorium in federal waters has been in place since 1987. In addition, commercial fishing of this species is prohibited in all GOM states except Mississippi. Consequently, the data sources that would be useful for assessing GOM red drum (e.g., commercial landings) are lacking (Powers et al., 2012). Therefore, despite a wealth of knowledge on population connectivity (e.g., Rooker et al., 2010), movement and recruitment (e.g., Burnsed et al., 2020), and

spawning (e.g., Lowerre-Barbieri et al., 2019), the red drum in the Gulf of Mexico is classified by the National Marine Fisheries Service as a “data-limited species” (SEDAR, 2016).

The reauthorization in 2006 of the Magnuson-Stevens Fishery Conservation and Management Act (Magnuson-Stevens . . . 2021) required development and implementation of annual catch limits for all federally managed stocks, a mandate that spurred significant advances in the development of methods for assessment of data-limited stocks (Newman et al., 2015). One of these methods, as implemented in the R package DLMtool (vers. 3.2.1; Carruthers and Hordyk, 2018), was recently used to assess a suite of data-limited species in the GOM, including the lane snapper (*Lutjanus synagris*), wenchman (*Pristipomoides aquilonaris*), yellowmouth grouper (*Mycteroperca interstitialis*), speckled hind (*Epinephelus drummond-hayi*), snowy grouper (*Hyporthodus niveatus*), almaco jack (*Seriola rivoliana*), lesser amberjack (*S. fasciata*), and red drum (SEDAR, 2016). During this assessment, at least one method for data-limited species was identified as having preferable performance compared to the status quo for every species examined, with the notable exception of red drum (SEDAR, 2016). Therefore, despite new tools tailored to the assessment of data-limited species and a wealth of information about the population biology and ecology of red drum, the results from this assessment were not recommended for providing management advice for red drum (SEDAR, 2016).

Careful consideration of existing data sets can improve our ability to assess stocks like the GOM stock of red drum. Specific data recommendations from the most recent assessment of red drum include 1) expansion of efforts to collect samples, for analysis of age and length, at varying sizes, seasons, months, and locations, particularly for offshore fish; 2) identification or optimization of fishery-independent surveys to characterize relative abundance in federal waters; and 3) exploration of ways to increase data collection from existing fishery-independent surveys (SEDAR, 2016). To those ends, the goals of this study were to combine data from fishery-independent surveys operating throughout the year and across the continental shelf to produce up-to-date overall and sex-specific growth models, update estimates of the instantaneous natural mortality rate ( $M$ ), generate standardized indices of relative abundance, and provide predictions of habitat suitability for red drum in the north-central GOM, with the expectation that the results of these efforts can be used to optimize future fishery-independent surveys.

## Materials and methods

### Data collection

Catch data for adult red drum were collected during fishery-independent bottom longline surveys conducted in all seasons in the north-central GOM during 2006–2018

(Fig. 1). The locations for bottom longline surveys were selected by using a stratified-random sampling design and were sampled following standardized methods described in Drymon et al. (2013, 2020). Briefly, the mainline consisted of 1.85 km (1 nmi) of 4-mm monofilament (545 kg test) that was set with 100 gangions. Gangions consisted of a longline snap and a 15/0 circle hook baited with Atlantic mackerel (*Scomber scombrus*). Each gangion was made of 3.66 m of 3-mm monofilament (320 kg test). All sets were soaked for 1 h, and mid-set measurements of surface and bottom temperatures (in degrees Celsius), salinity, and bottom dissolved oxygen (in milligrams per liter), as well as of depth at the start and end of each set (in meters), were recorded. During the retrieval of the bottom longline, all red drum encountered were measured to the nearest millimeter (maximum total length [TL]), weighed, and retained, and their sex was determined. Sagittal otoliths were extracted for age and growth analyses. Catch data were converted to catch per unit of effort (CPUE), expressed as the number of individuals per 100 hooks per hour.

To augment the samples of adult red drum from the bottom longline survey, smaller red drum were collected from the monthly gill-net survey of the Alabama Department of Conservation and Natural Resources, Marine Resources Division, during 2006–2018; these additional samples were aged. This survey includes areas of coastal Alabama from eastern Mississippi Sound to western Perdido Bay and Mobile Bay (Fig. 1) (Livernois et al., 2020). The gill-net survey of the Marine Resources Division involves 2 different nets: a small-mesh gill net and a large-mesh gill net. The small-mesh gill net consists of 5 panels that are 45.0 m long by 2.4 m deep, each containing stretch meshes in sizes of 5.1–10.2 cm. The large-mesh gill net consists of 4 panels that are also 45.0 m long by 2.4 m deep, with stretch meshes in sizes of 11.4–15.2 cm. Red drum caught in either gill net were measured to the nearest millimeter (maximum TL) and weighed, and their sex was determined. Sagittal otoliths were extracted for age and growth analyses.

For fish of all ages combined (from both longline and gill-net surveys), 2-sample Kolmogorov–Smirnov tests were used to examine differences in length and weight distributions between sexes. Some red drum collected with longlines were not measured for TL. For red drum from longline surveys that had both maximum total and fork length (FL) measurements, linear regression was used to examine the relationship of maximum TL to FL, resulting in this equation:

$$TL = 1.04(FL) + 23.53, \quad (1)$$

where TLs and FLs are expressed in millimeters (number of samples [ $n$ ]=346, coefficient of multiple determination [ $R^2$ ]=0.96). This regression was used to estimate the TLs of red drum from the longline survey that were lacking a maximum TL measurement ( $n$ =238). Differences in sex ratio were tested by using a chi-square test (Pearson, 1900) against an expected 1:1 male-to-female ratio.

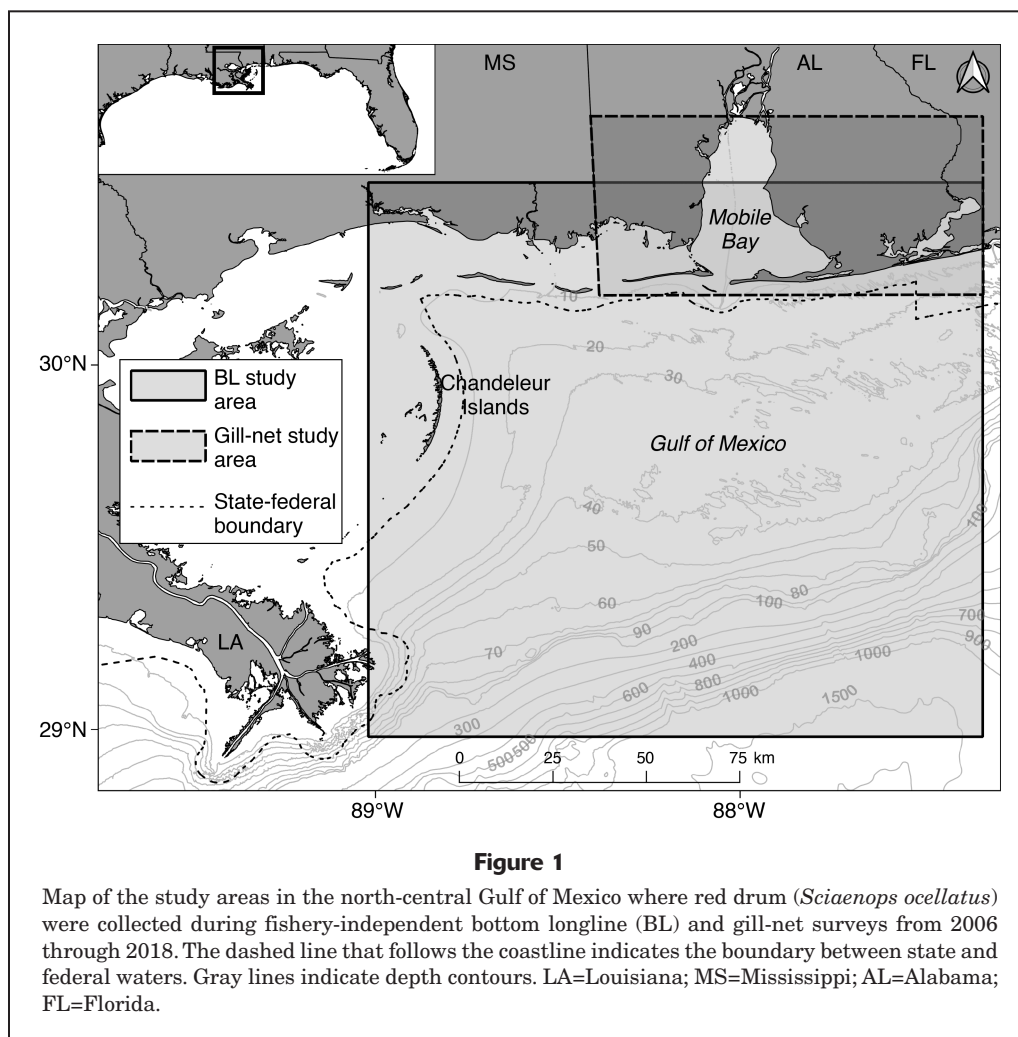


**Figure 1**

Map of the study areas in the north-central Gulf of Mexico where red drum (*Sciaenops ocellatus*) were collected during fishery-independent bottom longline (BL) and gill-net surveys from 2006 through 2018. The dashed line that follows the coastline indicates the boundary between state and federal waters. Gray lines indicate depth contours. LA=Louisiana; MS=Mississippi; AL=Alabama; FL=Florida.

### Otolith processing and aging

All otoliths were processed following procedures detailed in Powers et al. (2012) and VanderKooy et al.<sup>1</sup> A portion of the fish aged in Powers et al. (2012) were also included in our study; however, these fish were aged again as part of this study for consistency. Once otoliths were processed, aging was conducted by 2 readers independently (without consultation between readers) and blindly (without knowledge of fish capture date or size). Each otolith section was viewed with an Olympus<sup>2</sup> SZX16 stereomicroscope (Olympus Corp., Tokyo, Japan) with transmitted light (brightfield illumination). The number of opaque zones was counted along the ventral edge of the sulcus acusticus. A margin code (1–4) was assigned to the otolith

margin, according to the otolith manual of the Gulf States Marine Fisheries Commission (VanderKooy et al.<sup>1</sup>).

Whole age, in years, was calculated for each fish according to guidelines of the Gulf States Marine Fisheries Commission. If the collection month was January–June and the margin code was 3 or 4, the whole age equaled the number of opaque zones, plus 1. If the collection month was October–December and the margin code was 1 or 2, the whole age equaled the number of opaque zones, minus 1. For all other combinations of capture month and margin code, the whole age equaled the number of opaque zones. Next, the number of days between the capture date and October 1 (the assumed birth date of red drum; Ditty, 1986) of the previous year was calculated. This number was then divided by the total number of days in the capture year, and the result was added to the whole age to yield the fractional age.

If the readers assigned different whole ages to any otolith, the readers consulted with each other or a third reader aged the otolith. If the 2 initial readers did not reach an agreement or if the third reader did not agree with 1 of the 2 initial ages, the otolith was excluded from further analysis. Average percent error was calculated for all whole ages to

<sup>1</sup> VanderKooy, S., J. Carroll, S. Elzey, J. Gilmore, and J. Kipp (eds.). 2020. A practical handbook for determining the ages of Gulf of Mexico and Atlantic Coast fishes, 3rd ed. Gulf States Mar. Fish. Comm., Publ. 300, 248 p. [Available from [website](#).]

<sup>2</sup> Mention of trade names or commercial companies is for identification purposes only and does not imply endorsement by the National Marine Fisheries Service, NOAA.

evaluate between-reader precision (Beamish and Fournier, 1981; Campana, 2001). Two-sample Kolmogorov–Smirnov tests were used to examine differences in fractional age distributions between sexes.

### Modeling growth

To estimate growth parameters for red drum in this study, the von Bertalanffy growth function (VBGF) was fit to female and male red drum and to red drum of unknown sex for the complete data set, the fishery-independent Marine Resources Division gill-net data set, and the bottom longline data set, by using the following equation (von Bertalanffy, 1938):

$$L_t = L_\infty (1 - e^{-K(t-t_0)}), \quad (2)$$

where  $L_t$  = the predicted TL in millimeters;

$L_\infty$  = the mean asymptotic length in millimeters;

$K$  = the Brody growth coefficient ( $\text{years}^{-1}$ );

$t$  = the time (fractional age) in years; and

$t_0$  = the hypothetical age in years at which length equals 0.

The VBGF was used to model sex-specific growth. Eight candidate versions of the VBGF were fit to the sex-specific fractional age data: a general version, where all 3 parameters ( $L_\infty$ ,  $K$ , and  $t_0$ ) could vary between sexes; 3 versions where 2 of the 3 parameters could vary between sexes; 3 versions where only 1 parameter could vary between sexes; and a common version where all 3 parameters were held constant between sexes (Ogle, 2016; Nelson et al., 2018; Jefferson et al., 2019). Akaike information criterion (AIC) values were used to rank these models on the basis of fit and to identify the best-fitting version (Akaike, 1998; Katsanevakis and Maravelias, 2008; Ogle, 2016). All growth parameters were modeled in statistical software R, vers. 4.1.0 (R Core Team, 2021), with the add-on packages FSA (vers. 0.9.1; Ogle et al., 2021) and nlstools (vers. 1.0-2; Baty et al., 2015).

### Estimating mortality

By using whole ages of fish sampled in bottom longline surveys, an age-based catch curve (Chapman and Robson, 1960) was created for calculating total mortality; however, graphical examination of the catch curve revealed that critical assumptions necessary for estimating instantaneous total mortality had been violated (Tuckey et al., 2007; Smith et al., 2012). Specifically, red drum did not appear to fully recruit to the gear until age 20; therefore, any mortality estimates generated from this catch curve would not be representative of the stock. Although total mortality estimates were unattainable,  $M$  was calculated by using 3 empirical methods (Then et al., 2015; Ogle, 2016):

1. Hoenig<sub>fishes</sub>: Hoenig's (1983) log-transformed linear regression for fish species,

$$M = e^{1.46 - 1.01 \log_e(t_{\max})}, \quad (3)$$

where  $t_{\max}$  = the maximum age of the animal in years;

2. the Hoenig<sub>nl</sub> (nonlinear least squares) estimator (Then et al., 2015),

$$M = 4.899t_{\max}^{-0.916}; \text{ and} \quad (4)$$

3. the Pauly<sub>nl-T</sub> (nonlinear least squares, omitting temperature) estimator (Pauly, 1980; Then et al., 2015),

$$M = 4.118K^{0.73}L_\infty^{-0.333}, \quad (5)$$

where  $K$  and  $L_\infty$  are parameters from the combined VBGF. All mortality analyses were conducted with FSA in R.

### Relative abundance

Yearly changes in CPUE for red drum sampled during bottom longline surveys were examined by generating a nominal index of relative abundance. To standardize the index of relative abundance, a negative binomial generalized linear model (Hardin and Hilbe, 2007) was fit to the CPUE data by using the glmmTMB package (vers. 1.1.2; Brooks et al., 2017) in R. Abiotic variables thought to influence CPUE were added to the model by using forward stepwise model selection. Akaike information criterion values were used to identify the best-fitting model. Model fit was examined by using the DHARMA package (vers. 0.4.3; Hartig, 2021) in R to check for uniformity, outliers, dispersion, and zero inflation. Multicollinearity was tested by using the performance package (vers. 0.7.3; Lüdtke et al., 2021) in R, with variance inflation factors less than 10 signifying low correlation (Dormann et al., 2013). To create a standardized yearly index, the abiotic variables thought to influence CPUE were set to their median values.

### Spatial analysis

The index of relative abundance generated as described above was used to examine trends in relative abundance of red drum. First, minimum distance from shore (in kilometers) was calculated in QGIS, vers. 3.8.1 (QGIS Development Team, 2019). Then, nominal CPUE was calculated for 4 discrete areas: <3 nmi from shore (i.e., state waters), 3–6 nmi from shore, 6–9 nmi from shore, and >9 nmi from shore. Finally, a one-way analysis of variance, followed by a Tukey's multiple-pairwise-comparison test, was used to test for differences in nominal CPUE between these 4 areas. Age and length were examined in relation to distance from shore to identify the composition of red drum vulnerable to recreational fishermen in state waters versus that of those protected in federal waters.

### Habitat modeling

Boosted regression trees (BRTs) were used to describe the relationships between the CPUE of red drum from bottom longline surveys and environmental variables potentially influencing distribution and abundance. Specifically, BRTs were fit for 3 seasons (meteorological spring, summer, and autumn); winter data were not included in BRT analysis



given that few red drum were captured ( $n=35$ ) and effort was relatively low (70 stations). Boosted regression trees use machine learning to fit complex, nonlinear relationships and to offer predictive advantages over generalized linear or additive models. For a complete description of BRTs and the methods used in this study, see Drymon et al. (2020).

Results of preliminary analyses indicate a high proportion of zero values (i.e., zero-inflated data). To account for the preponderance of zeros, a 2-step (i.e., delta or hurdle) process was chosen to model catch data. Probability of presence and absence was modeled by using a BRT with a binary distribution, and continuous non-zero (i.e., abundance) probability was modeled by using a BRT with a Gaussian distribution. Because the catch data also contain some instances of anomalously high catch (i.e., long-tailed data), non-zero data were natural log-transformed. Predictions were reverse log-transformed so that the final model is a product of the binary and Gaussian BRTs (Lo et al., 1992).

Sixteen variables with data from multiple sources were considered for the BRTs (see table 1 in Drymon et al., 2020). Although data for some variables (e.g., temperature, salinity, and dissolved oxygen) were collected on-site during bottom longline sampling, all predictor data were obtained following methods outlined in Drymon et al. (2020) to facilitate comparisons with previous habitat modeling in the same region. Surface and bottom temperatures (in degrees Celsius), salinity, and 3-dimensional surface and bottom current velocities (surface, northward, and upward, in meters per second), as well as sea-surface height (in meters), were obtained from the Hybrid Coordinate Ocean Model data server (4-km resolution; HYCOM consortium, available from [website](#), accessed January 2020). Bottom dissolved oxygen (in milligrams per liter) was obtained from Gulf of Mexico Hypoxia Watch maps (NOAA National Centers for Environmental Information, available from [website](#), accessed January 2020) and interpolated across ~100–250 survey stations (the number of stations varied by year). Depth (in meters) and substrate grain size (in millimeters) were obtained from the Coastal Relief Model bathymetry for the Gulf of Mexico (resolution of 0.33 arc seconds or ~10 m; Buczkowski et al., 2006; U.S. Geological Survey, *gmx\_grd.zip*, available from [website](#)). Day length (in minutes) was calculated in R by using code by S. Dedman (available from [GitHub](#), accessed January 2020).

Given the quantity of potential predictor data considered within the BRTs, some degree of spatial autocorrelation was anticipated (e.g., between distance from shore and depth, between surface and bottom temperatures); however, BRTs are robust despite autocorrelation among independent variables (Abeare, 2009). All BRTs were fit by using the package *gbm.auto* (vers. 1.4.1; Dedman et al., 2017) in R. Learning rate, bag fraction, and tree contribution are parameters that are used in concert to determine minimum predictive error (Elith et al., 2008). These parameters were optimized by using *gbm.auto* for the model run for each season.

## Model performance and interpretation

The BRT modeling approach allowed automatic partitioning of the data into training and testing sets, at a ratio dictated by the bag fraction. Ten-fold cross validation was then performed, with the members of the training and testing sets randomized each time. Performance metrics included training and testing correlation, cross-validation deviance (and standard error [SE]), and correlation (and SE), as well as area under receiver-operator curve (AUC) (Hanley and McNeil, 1982) and its cross-validation and cross-validation SE for the binary models (Parisien and Moritz, 2009). The final Gaussian fitted functions from the BRT were visualized by using marginal effect plots to indicate the effect of a particular variable on the response after accounting for the average effects of other model variables (Elith et al., 2008).

## Habitat suitability

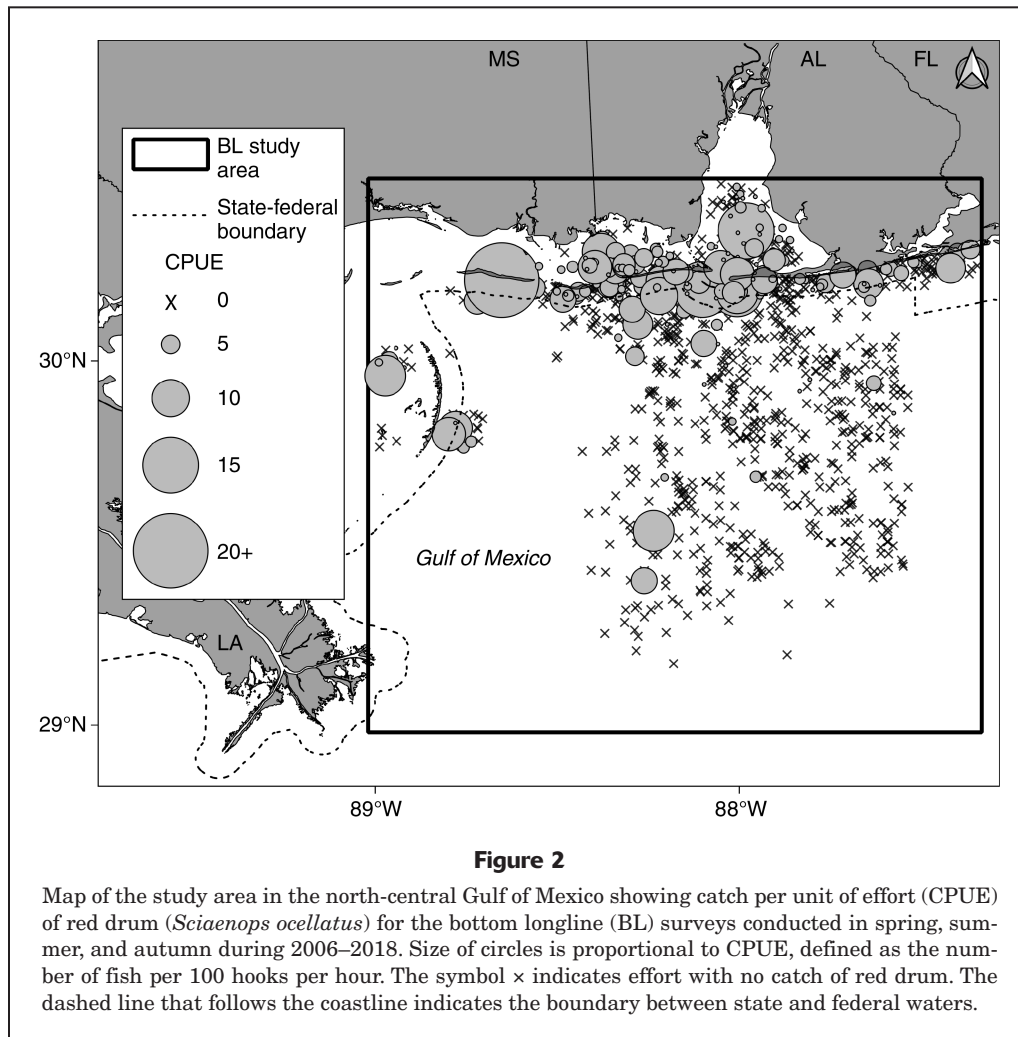
The distribution of suitable habitat was predicted by using the BRTs described previously. Environmental data for model predictions were obtained as detailed previously, except that Hybrid Coordinate Ocean Model data were extracted for one representative date per season (the monthly groupings for the seasons were March–May, June–August, and September–November). Representative dates for environmental data were selected by ranking the absolute value of the differences between values for all sites for all variables against the mean for those variables, then by identifying the date within each season that most closely matched those values. The BRTs then were used to predict CPUE values for each 2-by-2-km cell. These values were then mapped in QGIS by using the heatmap setting to produce color points weighted by the predicted abundances generated from the BRT. By using *gbm.auto*, the coefficient of variance was calculated for the predicted abundance values for each 2-by-2-km cell to represent model variance.

## Results

### Catch data

Between May 2006 and November 2018, 1296 bottom longline sets were conducted and 815 red drum were caught (Fig. 2), with 741 of those red drum measured and 472 fish kept for otolith collection. Approximately 100 stations were sampled each year (mean: 100 stations [standard deviation 22]; range: 80–143 stations), and survey effort (number of sets) was relatively well distributed across the 3 seasons examined in the BRTs: spring (460 sets), summer (405 sets), and autumn (361 sets). Red drum caught on bottom longlines were primarily encountered in state waters across all seasons (Fig. 2) and were exclusively larger than the size at 50% maturity reported by Bennetts et al. (2019) (Fig. 3A).

To supplement the otoliths taken from the 472 red drum retained from the bottom longline surveys, otoliths from



an additional 709 red drum captured in gill nets were analyzed; therefore, a total of 1181 red drum were used for age and growth analyses. Of these fish, 392 red drum were female, 369 fish were male, and 420 fish were of unknown sex. The female-to-male ratio was 1.06:1.00 and did not differ significantly from a 1:1 ratio ( $\chi^2=0.70$ ,  $df=1$ ,  $P=0.40$ ). Total lengths of red drum were 80–1102 mm (Fig. 3B). The average TL of all fish examined (those caught with bottom longlines and gill nets combined) was 619.13 mm (SE 8.22). Results from Kolmogorov–Smirnov tests indicate that females were significantly longer ( $D=0.20$ ,  $P<0.01$ ) and heavier ( $D=0.18$ ,  $P<0.01$ ) than males.

### Age

Ages were assigned to 1178 red drum. Otoliths from the remaining 3 fish (0.25% of all red drum from which otoliths were taken) were deemed unreadable and were omitted from further analysis. Four fish had no length measurements and were also omitted from further analysis. The between-reader percent agreement was 93.46%, and the between-reader average percent error was 4.52%;

these estimates are largely driven by differences in the margin codes assigned to age-0 fish. Whole ages ranged from 0 to 36 years, and fractional ages ranged from 0.37 to 36.53 years. The maximum age of both sexes was 36 years; however, results of Kolmogorov–Smirnov tests indicate that fractional age distributions differed significantly by sex ( $D=0.15$ ,  $P<0.01$ ). The mean ages of females and males were 11.72 and 9.90 years, respectively.

### Growth and mortality

The VBGF for all age data combined (including females, males, and fish of unknown sex) is as follows:

$$L_t = 950.45(1 - e^{-0.31(t - (-0.26))}) \text{ (Fig. 4A).} \quad (6)$$

For the sex-specific data, the model version that allowed  $L_\infty$  and  $t_0$  to vary by sex best fit the data. This model version was followed closely by the version in which  $L_\infty$  and  $K$  vary (difference in AIC values [ $\Delta AIC$ ] between these 2 models: 1.7) and the version that allowed all parameters to vary ( $\Delta AIC$  for the best fit version and this version: 1.7). On the basis of predictions from the best-fit model, females

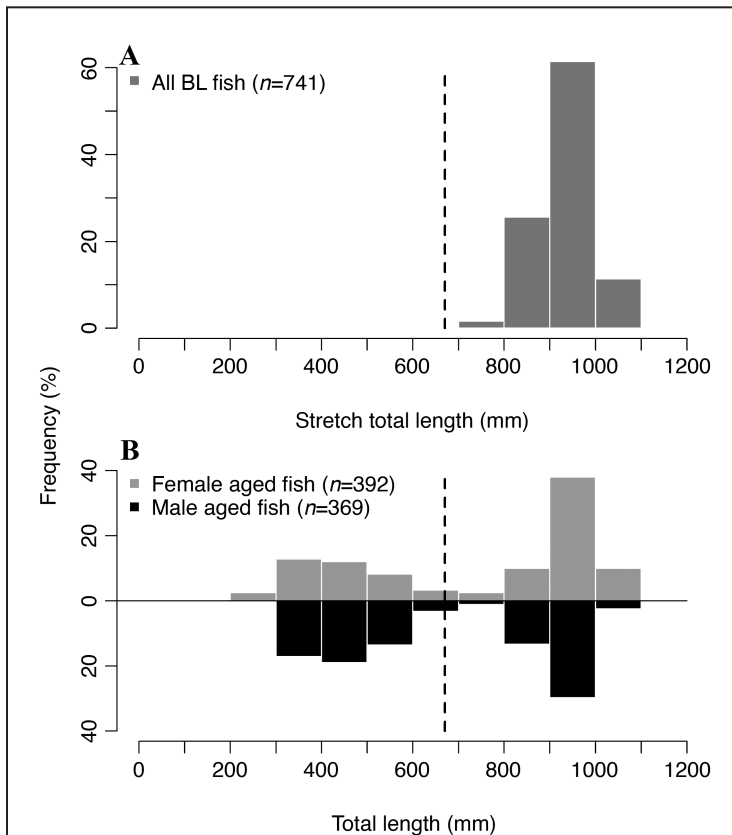


**Figure 3**

Length–frequency distributions for (A) red drum (*Sciaenops ocellatus*) encountered during bottom longline (BL) surveys (sexes combined) and (B) red drum encountered during BL and gill-net surveys (by sex) in the north-central Gulf of Mexico from 2006 through 2018. The vertical dashed line represents size at 50% maturity, reported by Bennetts et al. (2019).  $n$ =number of samples.

have a higher  $L_{\infty}$  value compared with that of males. The VBGF versions for female (F) and male (M) red drum, respectively, are as follows:

$$L_{t(F)} = 969.63(1 - e^{-0.30(t - (-0.35))}); \text{ and} \quad (7)$$

$$L_{t(M)} = 932.71(1 - e^{-0.30(t - (-0.45))}) \text{ (Fig. 4B)}. \quad (8)$$

All VBGF parameter estimates from this study are listed in Table 1. Estimates of  $M$  were 0.12 for the Hoenig<sub>fishes</sub> method, 0.14 for the Hoenig<sub>nlis</sub> method, and 0.39 for the Pauly<sub>nlis-T</sub> method.

#### Relative abundance

The final version of the negative binomial generalized linear model included variables for year, depth, surface temperature, dissolved oxygen, and bottom salinity. The variables for latitude, longitude, bottom temperature, surface salinity, and day length were also tested but were excluded from the final version of the model. Model fit was deemed appropriate because the model did not

suffer from deviations from uniformity, outliers (Suppl. Fig. 1), dispersion ( $P=0.92$ ), or zero inflation ( $P=0.87$ ). The results of the variance inflation factor analysis indicate a lack of multicollinearity, given that all variance inflation factors were less than 2. The variable for year was not significant ( $P=0.13$ ), and there were no trends within the standardized index (Fig. 5), indicating that the declines in the nominal CPUE data for 2007–2010 reflect increases in offshore sampling effort beginning in 2010 rather than changes in relative abundance of red drum.

#### Spatial analysis

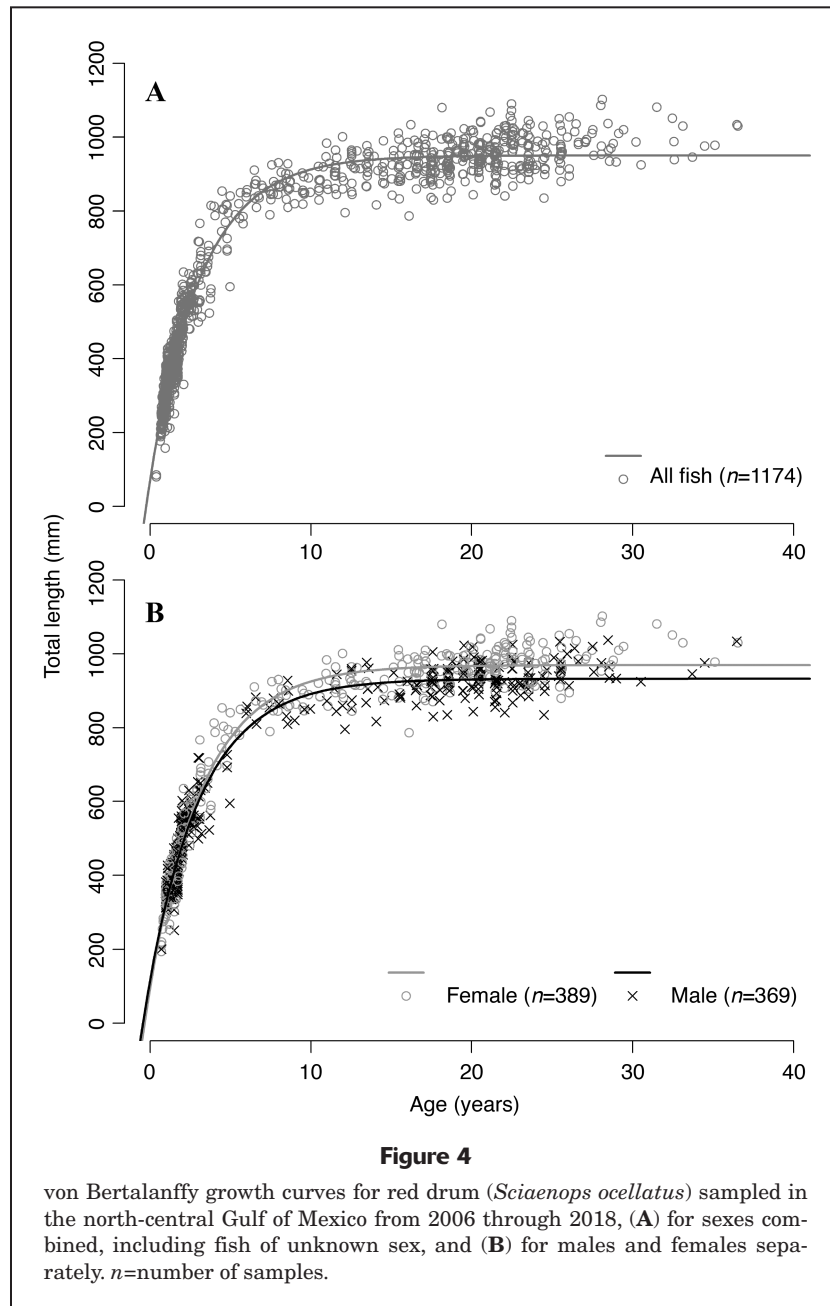
During 2006–2018, bottom longline sets were distributed fairly evenly between state (46%) and federal (54%) waters. Nominal CPUE was highest less than 3 nmi from shore (1.13 [SE 0.10], 602 stations), followed by 3–6 nmi from shore (0.72 [SE 0.18], 103 stations), 6–9 nmi from shore (0.35 [SE 0.19], 58 stations), and greater than 9 nmi from shore (0.08 [SE 0.03], 533 stations). The one-way analysis of variance found that distance from shore was significant ( $P<0.01$ ). The results from the Tukey's multiple-pairwise-comparison test indicate that nominal CPUE was significantly higher less than 3 nmi from shore compared with 6–9 nmi from shore ( $P<0.01$ ) and greater than 9 nmi from shore ( $P<0.01$ ). Nominal CPUE was also significantly higher 3–6 nmi from shore than greater than 9 nmi from shore ( $P<0.01$ ). Both ages ( $D=0.41$ ,  $P<0.01$ ) and length distributions ( $D=0.42$ ,  $P<0.01$ ) were significantly different for red drum caught in state versus federal waters. Notably, fish were older and larger in state waters (average age of 18 years and average total length of 938 mm) than in federal waters (average age of 12 years and average total length of 887 mm). Further examination revealed a negative correlation between age and distance from shore (coefficient of correlation  $[r]=-0.239$ ,  $P<0.01$ ) and between size and distance from shore ( $r=-0.274$ ,  $P<0.01$ ).

#### Model performance and interpretation

Model performance was assessed for all red drum across the 3 sampling seasons: spring, summer, and autumn. The AUC scores for training data were high across all seasons (0.90), indicating “very good” model performance according to criteria defined in Lane et al. (2009) (Table 2). Cross-validated AUC scores were 0.85–0.86 (SE 0.01), indicating that model overfitting was negligible (Hijmans and Elith, 2013).

#### Habitat suitability

Across all seasons, northward velocity of the surface current, surface temperature, and depth were the 3 most influential predictors of abundance of red drum (Table 2).



In particular, red drum had a preference for surface current northward velocities greater than 0 m/s, with high preferences for velocities greater than 0.1 m/s (Fig. 6, A, D, and G). Preferences for surface temperatures less than 22°C (Fig. 6, B, E, and H) and depths between 5 and 17 m (Fig. 6, C, F, and I) were also apparent. These predictors were consistent across seasons. In general, the most suitable habitat for red drum was predominately within state waters. A seasonal shift in predicted habitat suitability was detected, indicating that red drum prefer shallow (<10 m) habitats in the spring and autumn and deep (>30 m) waters during the summer (Fig. 7). Coefficients of variance of the predicted relative abundance were low, but were highest in deep waters (Suppl. Fig. 2). Because all fish in the BRT analysis were larger than the estimated size at 50% maturity (Fig. 3A), we are confident that these results do not confound localized spatial preferences with life history shifts in habitat use.

## Discussion

Our findings, based on a large sample size and broad size distribution, support results of previous studies indicating that the red drum is a relatively long-lived, slow-growing species in the GOM. Perhaps not surprisingly, our findings are most similar to those of Bennetts et al. (2019); 3-parameter VBGFs were used in both studies to model sex-specific growth from a similar number and size range of fish collected in Mississippi and Alabama. However, the maximum age in our study is notably older than the maximum age reported by Bennetts et al. (2019) (36 years

**Table 1**

Mean estimates for parameters of the von Bertalanffy growth function, by sex, based on age data for red drum (*Sciaenops ocellatus*) collected from 2006 through 2018 during fishery-independent bottom longline and gill-net surveys in the north-central Gulf of Mexico. Parameters include mean asymptotic length ( $L_{\infty}$ ), Brody growth coefficient ( $K$ ), and hypothetical age at which length equals 0 ( $t_0$ ). The category for sexes combined includes fish of unknown sex. Standard errors of the mean (SE) are provided in parentheses.

Sex	$L_{\infty}$ (mm)	$K$ (years <sup>-1</sup> )	$t_0$ (years)
Combined	950.45 (2.35)	0.31 (0.01)	-0.26 (0.03)
Female	969.63 (3.42)	0.30 (0.01)	-0.35 (0.05)
Male	932.71 (3.78)	0.30 (0.01)	-0.45 (0.06)



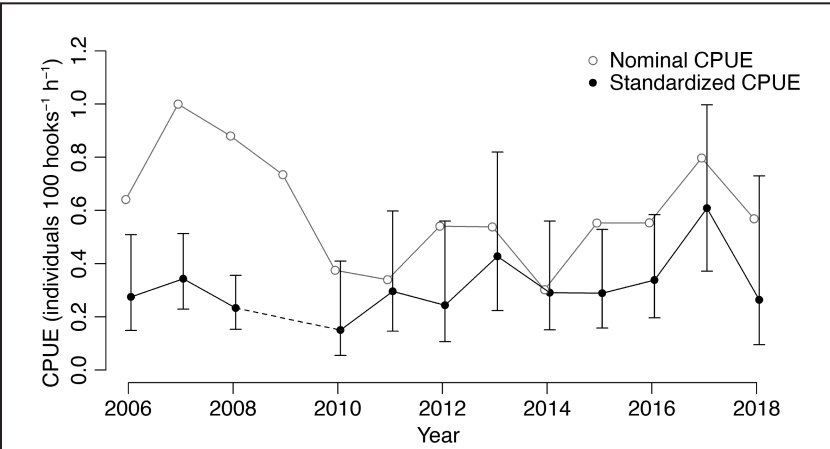


Figure 5

Nominal and standardized catch per unit of effort (CPUE) of red drum (*Sciaenops ocellatus*) from bottom longline surveys conducted in the north-central Gulf of Mexico during 2006–2018. A mean of 100 stations (standard deviation 22) were sampled per year (range: 80–143 stations). Median values are shown in the index standardized by fitting a negative binomial generalized linear model to the CPUE data. For 2009, there is no standardized CPUE estimate because of a lack of positive catch data with corresponding data for abiotic variables from that year. Error bars indicate 95% confidence intervals of standardized CPUE.

versus 31 years), a difference that illustrates the importance of sampling enough large, presumably old individuals. Specifically, we collected more than 4 times more individuals larger than 1000 mm TL than Bennetts et al. (2019); 2 of these fish, 1 male and 1 female, were assigned ages of 36 years. Although fish older than 36 years are likely rare off Mississippi and Alabama, future efforts to model age and growth for red drum should consider collections that span the entirety of the range of the species. Future research also should account for the effects of gear selectivity, temporal or spatial changes in age structure, variable recruitment, and unexplained variance arising from individuals of undetermined sex, all of which are potential sources of bias in growth model parameters in this study.

Despite the large sample size and broad size distribution of red drum captured by using 2 fishery-independent gear types, individuals between 600 and 800 mm TL (ages 3–6) were notably rare in our study. Interestingly, it is in this size range that red drum in this region undergo maturation, according to mean estimates of size and age at maturity from Bennetts et al. (2019). Specifically, mean age at 50% maturity for males and females is approximately 3 years, with fully mature individuals (spawning capable and elevated gonadosomatic index) undetected until ages 5 and 6 (Bennetts et al., 2019). Therefore, although a multi-panel gill net can adequately sample fish of ages 0–2 and the bottom longline can adequately sample fish of age 7 and older, fish between the ages of 3 and 6 years are not selected by either gear type. Similar size selectivity has been reported for red drum off the West Florida Shelf. Using 3 fishery-independent gear types (haul seine, trammel net, and purse seine), Winner et al. (2014) demonstrated that red drum that were 600–800 mm TL were not well

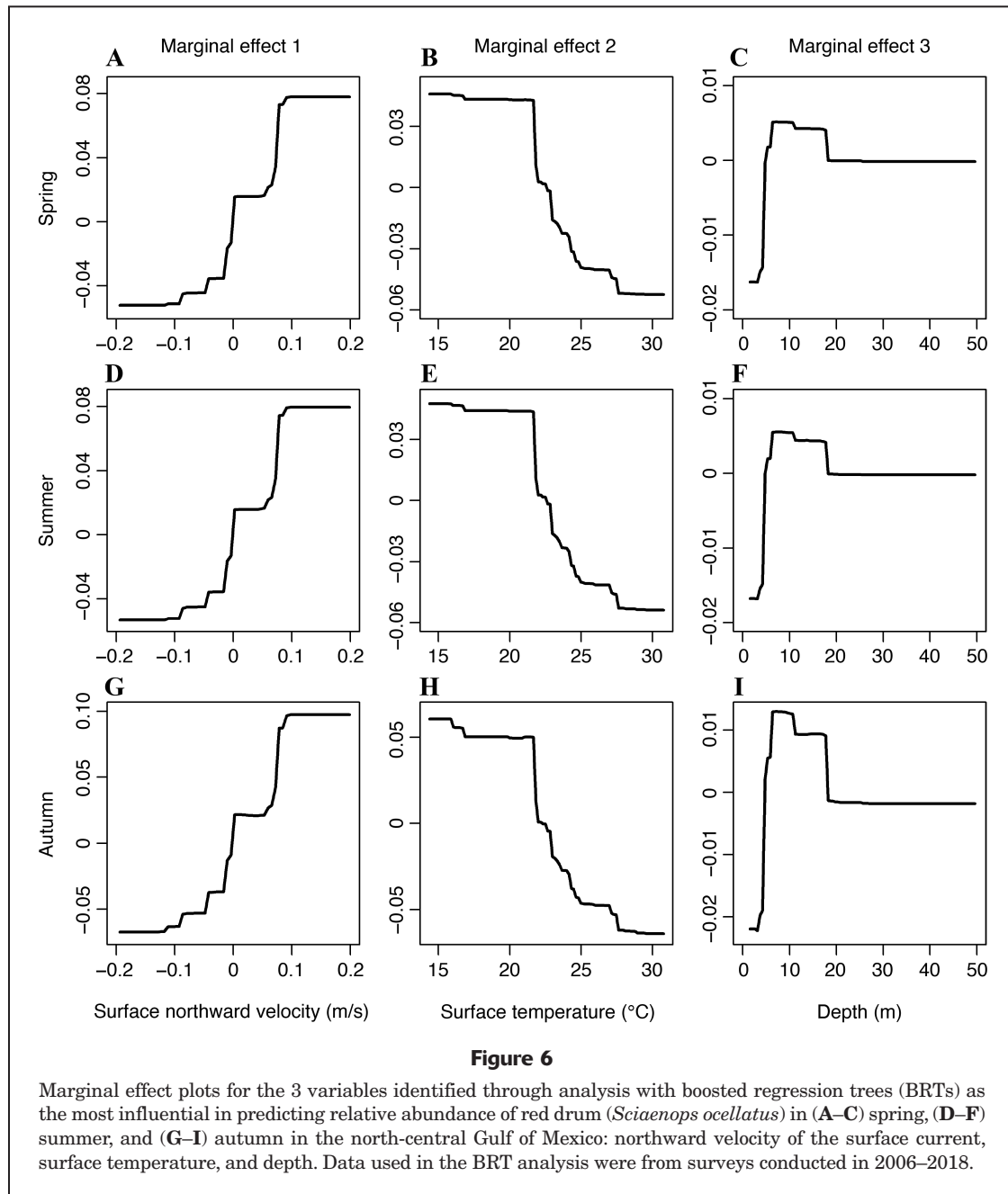
represented in the catch in either haul seines or purse seines, yet they were dominant in trammel-net surveys. These examples illustrate that population dynamics are difficult to assess for red drum and that multiple gear types are needed to describe population dynamics across all life stages of this species.

Surprisingly, a comprehensive review of life history studies of red drum revealed that recent age-based estimates of  $M$  are not available for this species (SEDAR, 2016). During the most recent stock assessment, it was concluded that the updated Hoenig equation using longevity (Then et al., 2015) was the most robust approach for red drum. Our estimate of annual  $M$  based on the Then et al. (2015) approach was 0.14 year<sup>-1</sup>, a rate that is similar to the range of values used in

Table 2

Percentage of contribution of the 3 variables identified through analysis with boosted regression trees as the most influential on relative abundance of red drum (*Sciaenops ocellatus*) in the north-central Gulf of Mexico between 2006 and 2018. The area under receiver-operator-curve (AUC) and cross-validated (CV) AUC scores, with standard errors (SEs), were used to assess the model's ability to discriminate between species presence and absence.

Season	Training data AUC score	CV AUC score (SE)	Marginal Effect 1		Marginal Effect 2		Marginal Effect 3	
			Variable	%	Variable	%	Variable	%
Spring	0.90	0.86 (0.01)	Northward velocity of surface current	26.2	Surface temperature	20.7	Depth	14.7
Summer	0.90	0.85 (0.01)	Northward velocity of surface current	25.8	Surface temperature	20.4	Depth	14.6
Autumn	0.90	0.86 (0.01)	Northward velocity of surface current	25.8	Surface temperature	20.4	Depth	14.4



the assessment ( $0.16\text{--}0.18\text{ year}^{-1}$ ). Unfortunately, the current approach for stock assessments (DLMtool; Carruthers and Hordyk, 2018) does not allow for age-dependent estimates of  $M$ . The inability to model age-dependent mortality is potentially problematic for red drum because fishing pressure is higher for juveniles, which likely experience different  $M$  than that experienced by older individuals. As the red drum becomes less data-limited, development of the ability to account for age-based differences in  $M$  should be prioritized.

The development of a Gulf-wide index of relative abundance generated from fishery-independent bottom longline surveys is critical for future assessments of

red drum. During the last stock assessment, 6 potential methods were considered for generating catch advice. The only method to meet the performance criteria was Islope, which is solely based on an index of relative abundance (Carruthers and Hordyk, 2018). For GOM red drum, the index of relative abundance deemed most representative of the adult spawning stock was the index based on data from our bottom longline survey. Therefore, the index of relative abundance generated in this study is an important step toward producing catch advice for this data-limited species. This index indicates that the relative abundance of red drum has varied little over the past 13 years. However, given the long life span of red drum,

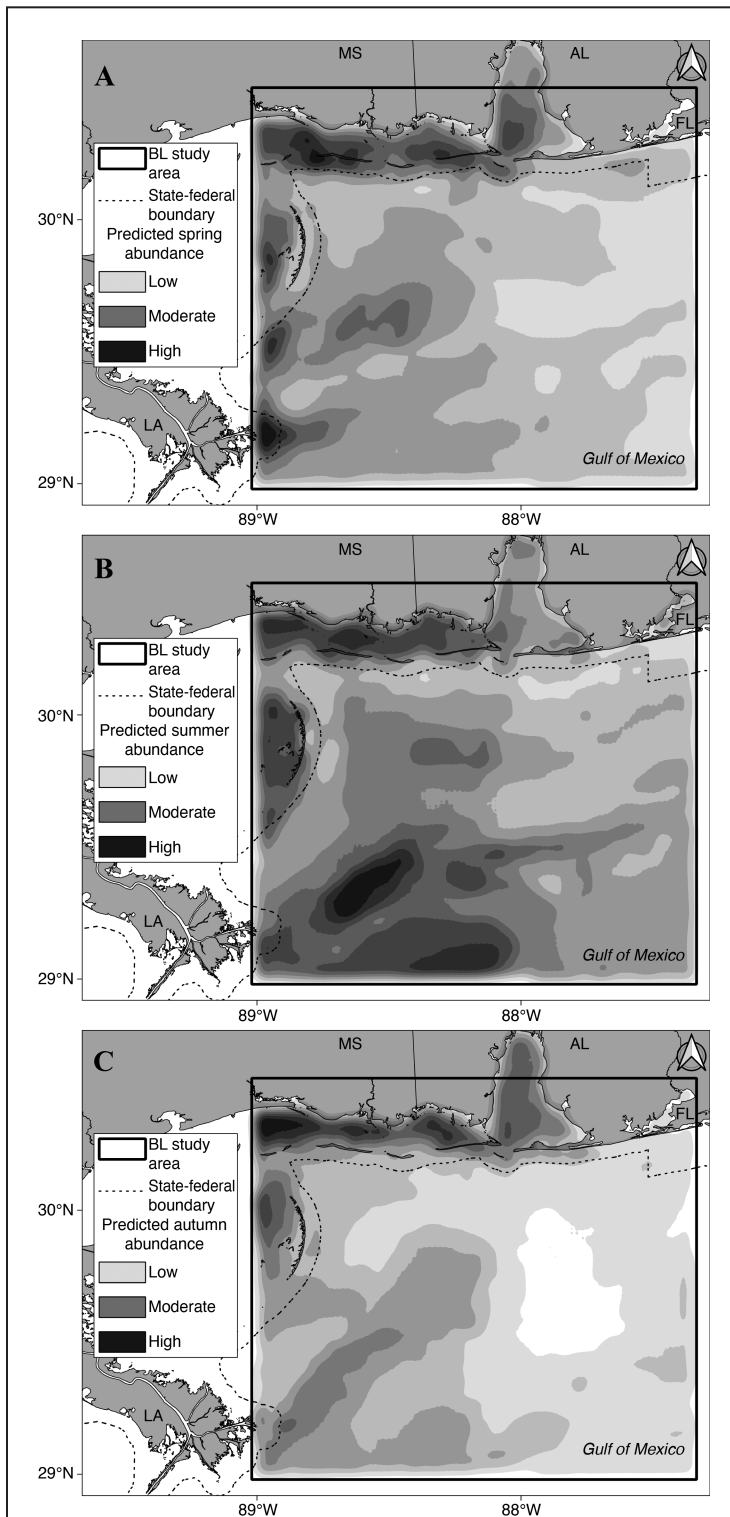


**Figure 7**

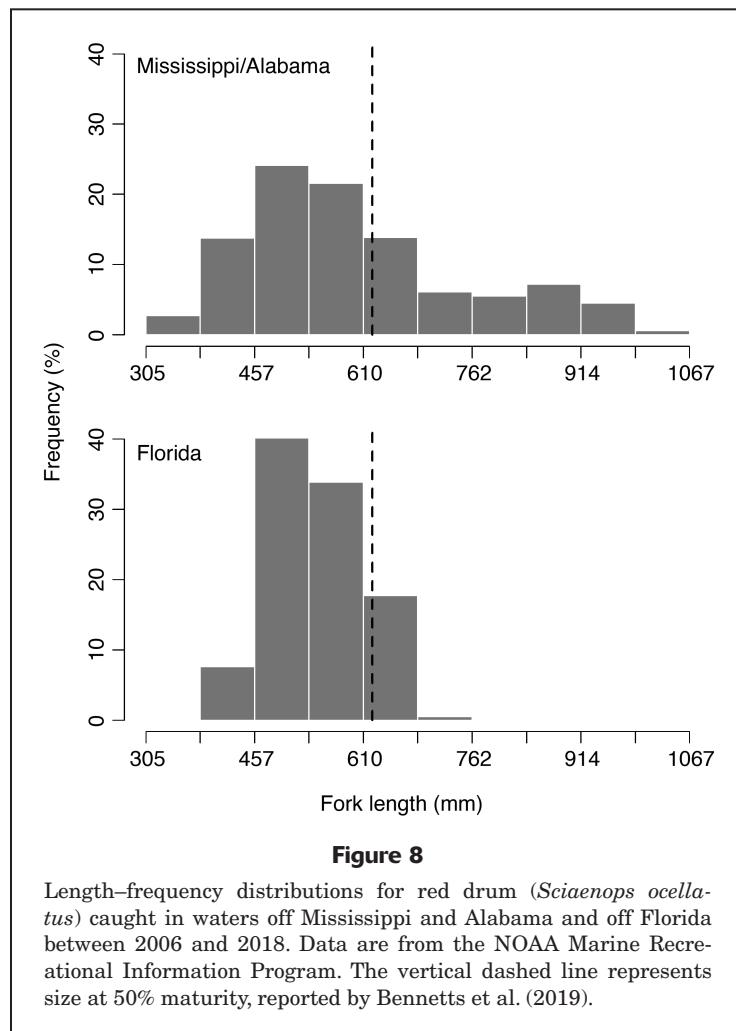
Maps of the study area showing predicted relative abundance from boosted regression trees (BRTs) for red drum (*Sciaenops ocellatus*) collected in (A) spring, (B) summer, and (C) autumn during bottom longline (BL) surveys in the north-central Gulf of Mexico. Light shades indicate areas of low predicted abundance, and dark shades indicate areas of high predicted abundance. The dashed line that follows the coastline indicates the boundary between state and federal waters. Data used in the BRT analysis were from surveys conducted in 2006–2018.

changes in relative abundance for this species are likely to be delayed and gradual. Consequently, continued fishery-independent monitoring is essential, both for characterizing changes in the population and for increasing the stability of catch advice generated from future stock assessments that apply the Islope approach (Sagarese et al., 2019).

Management of red drum in the GOM currently relies on each GOM state meeting an escapement goal (30%) of 4-year-old red drum (SEDAR, 2016). The premise of this management scheme is that most of these fish would enter the offshore adult population where the federal moratorium on GOM red drum protects the adult spawning stock. However, CPUE for adult red drum in the north-central GOM has been substantially higher in state waters than in federal waters (Powers et al., 2012). Similar differences in CPUE between jurisdictions has been observed in other areas of the GOM (e.g., Winner et al., 2014) and along the east coast of Florida (Reyier et al., 2011), particularly from August through November when adults return to state waters to spawn (Lowerre-Barbieri et al., 2016, 2019). These individuals travel to natal areas where they are targeted within spawning aggregations (Burnsed et al., 2020).

Although state-level management of red drum is primarily focused on regulating the catch of juveniles by using slot limits, the current management plans for 4 out of 5 GOM states (i.e., all GOM states except Florida) also afford opportunities to keep a red drum larger than the slot limit. For example, landings data from the NOAA Marine Recreational Information Program (recreational fisheries statistics, available from [website](#), accessed September 2021) indicate that nearly 20% of red drum taken from Mississippi and Alabama state waters have been greater than 762 mm FL (30 in FL), whereas no fish larger than this size have been landed in Florida (Fig. 8). Our findings clearly indicate that off the coast of Alabama, the federal moratorium does not protect the larger, older age classes of red drum from exploitation. Adequately protecting these fish will require state management measures that either completely prohibit the catch of large individuals (e.g., as is done in Florida) or impose a tag system that allows a single over-slot fish per year (e.g., as is done in Texas).

The catch data support the outputs from the BRTs, and the results of BRT analysis indicate that adult red drum prefer inshore, state waters. It has been long established that schools of spawning red drum aggregate near tidal passes (Lowerre-Barbieri et al., 2008; Reyier et al., 2011); the results of our analysis indicate a mechanistic explanation for this observation, confirming the



GOM red drum. In addition to updated ages, growth models, and  $M$  estimates, the results of our investigation reveal that the adult spawning stock is not fully protected by the federal catch moratorium. Moreover, through use of our habitat suitability models, we identified factors that may predict suitable habitat for red drum in other regions of the GOM. Collectively, the findings from this study, in concert with those from future efforts to combine nearshore indices of relative abundance from standardized bottom longline surveys throughout the region (e.g., the surveys of the Southeast Area Monitoring and Assessment Program), will be critical for advancing the stock of red drum in the GOM from its status as data-limited.

### Acknowledgments

We thank Dauphin Island Sea Lab captains and crew, especially Captains T. Guoba and J. Wittmann, for their help with the bottom longline survey. We thank A. Kroetz, T. Spearman, T. Nelson, and others for their help with field collections, otolith processing, and aging. Thanks to the Marine Resources Division, Alabama Department of Conservation and Natural Resources, for collecting and sharing data on red drum from gill-net surveys. This work was conducted in accordance with Institutional Animal Care and Use Committee protocol no. 1562086 and was funded in part by the Gulf of Mexico Fishery Management Council.

importance of surface current velocity when defining suitable habitat for red drum. Temperature is also a well known and strong predictor of habitat use of red drum. In previous work in this region, bimodal peaks in relative abundance in the spring and autumn were documented as was the correspondence of these seasonal peaks to temperatures of 21°C and 20°C, respectively (Powers et al., 2012), which are consistent with the temperatures identified in this study as those preferred by red drum. On the basis of habitat suitability predictions from the BRTs, we speculate that during the summer, adult red drum may be using deep (>30 m), cool (~20°C) waters as a thermal refuge.

### Conclusions

Clearly, assessing a stock under a complete catch moratorium presents distinct challenges. Nonetheless, when the data typically used to assess the status of a stock (e.g., commercial catch data) are lacking, an opportunity exists to consider alternative data sources, which can sometimes provide new information about stock dynamics (Olney and Hoenig, 2001). Such is the case for

### Literature cited

- Abeare, S. M.  
2009. Comparisons of boosted regression tree, GLM and GAM performance in the standardization of yellowfin tuna catch-rate data from the Gulf of Mexico online [sic] fishery. M.S. thesis, 71 p. La. State Univ., Baton Rouge, LA. [Available from [website](#).]
- Akaike, H.  
1998. Information theory and an extension of the maximum likelihood principle. *In* Selected papers of Hirotugu Akaike (E. Parzen, K. Tanabe, and G. Kitagawa, eds.), p. 199–213. Springer, New York.
- Baty, F., C. Ritz, S. Charles, M. Brutsche, J.-P. Flandrois, and M.-L. Delignette-Muller.  
2015. A toolbox for nonlinear regression in R: the package nlstools. *J. Stat. Softw.* 66(5):1–21. [Crossref](#)
- Beamish, R. J., and D. A. Fournier.  
1981. A method for comparing the precision of a set of age determinations. *Can. J. Fish. Aquat. Sci.* 38:982–983. [Crossref](#)
- Bennetts, C. F., R. L. Leaf, and N. J. Brown-Peterson.  
2019. Sex-specific growth and reproductive dynamics of red drum in the northern Gulf of Mexico. *Mar. Coast. Fish.* 11:213–230. [Crossref](#)



- Berger, A. M., D. R. Goethel, and P. D. Lynch.  
2017. Introduction to “space oddity: recent advances incorporating spatial processes in the fishery stock assessment and management interface.” *Can. J. Fish. Aquat. Sci.* 74:1693–1697. [Crossref](#)
- Brooks, M. E., K. Kristensen, K. J. van Benthem, A. Magnusson, C. W. Berg, A. Nielsen, H. J. Skaug, M. Mächler, and B. M. Bolker.  
2017. glmmTMB balances speed and flexibility among packages for zero-inflated generalized linear mixed modeling. *R J.* 9(2):378–400. [Crossref](#)
- Buczkowski, B. J., J. A. Reid, C. J. Jenkins, J. M. Reid, S. J. Williams, and J. G. Flocks.  
2006. usSEABED: Gulf of Mexico and Caribbean (Puerto Rico and U.S. Virgin Islands) offshore surficial sediment data release. U.S. Geol. Surv. Data Ser. 146. Woods Hole Sci. Cent., Coast. Mar. Program, U.S. Geol. Surv., Woods Hole, MA. [Available from [website](#).]
- Burnsed, S. W., S. Lowerre-Barbieri, J. Bickford, and E. H. Leone.  
2020. Recruitment and movement ecology of red drum *Sciaenops ocellatus* differs by natal estuary. *Mar. Ecol. Prog. Ser.* 633:181–196. [Crossref](#)
- Campana, S. E.  
2001. Accuracy, precision and quality control in age determination, including a review of the use and abuse of age validation methods. *J. Fish Biol.* 59:197–242. [Crossref](#)
- Carruthers, T. R., and A. R. Hordyk.  
2018. The data-limited methods toolkit (DLM tool): an R package for informing management of data-limited populations. *Methods Ecol. Evol.* 9:2388–2395. [Crossref](#)
- Chapman, D. G., and D. S. Robson.  
1960. The analysis of a catch curve. *Biometrics* 16:354–368. [Crossref](#)
- Dedman, S., R. Officer, M. Clarke, D. G. Reid, and D. Brophy.  
2017. Gbm.auto: a software tool to simplify spatial modelling and marine protected area planning. *PLoS ONE* 12(12):e0188955. [Crossref](#)
- Ditty, J. G.  
1986. Ichthyoplankton in neritic waters of the northern Gulf of Mexico off Louisiana: composition, relative abundance, and seasonality. *Fish. Bull.* 84:935–946.
- Dormann, C. F., J. Elith, S. Bacher, C. Buchmann, G. Carl, G. Carré, J. R. G. Marquéz, B. Gruber, B. Lafourcade, P. J. Leitão, et al.  
2013. Collinearity: a review of methods to deal with it and a simulation study evaluating their performance. *Ecography* 36:27–46. [Crossref](#)
- Drymon, J. M., L. Carassou, S. P. Powers, M. Grace, J. Dindo, and B. Dzwonkowski.  
2013. Multiscale analysis of factors that affect the distribution of sharks throughout the northern Gulf of Mexico. *Fish. Bull.* 111:370–380. [Crossref](#)
- Drymon, J. M., S. Dedman, J. T. Froeschke, E. A. Seubert, A. E. Jefferson, A. M. Kroetz, J. F. Mareska, and S. P. Powers.  
2020. Defining sex-specific habitat suitability for a northern Gulf of Mexico shark assemblage. *Front. Mar. Sci.* 7:35. [Crossref](#)
- Elith, J., J. R. Leathwick, and T. Hastie.  
2008. A working guide to boosted regression trees. *J. Anim. Ecol.* 77:802–813. [Crossref](#)
- Goethel, D. R., T. J. Quinn II, and S. X. Cadrin.  
2011. Incorporating spatial structure in stock assessment: movement modeling in marine fish population dynamics. *Rev. Fish. Sci.* 19:119–136. [Crossref](#)
- Hanley, J. A., and B. J. McNeil.  
1982. The meaning and use of the area under a receiver operating characteristic (ROC) curve. *Radiology* 143:29–36. [Crossref](#)
- Hardin, J. W., and J. M. Hilbe.  
2007. Generalized linear models and extensions, 2nd ed., 387 p. Stata Press, College Station, TX.
- Hartig, F.  
2021. DHARMa: residual diagnostics for hierarchical (multi-level/mixed) regression models. R package, vers. 0.4.3. [Available from [website](#), accessed August 2021.]
- Hijmans, R. J., and J. Elith.  
2013. Species distribution modeling with R. In *Spatial data science with R*. R CRAN Proj., R Found. Stat. Comput., Vienna, Austria. [Available from [website](#).]
- Hoenig, J. M.  
1983. Empirical use of longevity data to estimate mortality rates. *Fish. Bull.* 82:898–903.
- Jefferson, A. E., R. J. Allman, A. E. Pacicco, J. S. Franks, F. J. Hernandez, M. A. Albins, S. P. Powers, R. L. Shipp, and J. M. Drymon.  
2019. Age and growth of gray triggerfish (*Balistes capriscus*) from a north-central Gulf of Mexico artificial reef zone. *Bull. Mar. Sci.* 95:177–195. [Crossref](#)
- Katsanevakis, S., and C. D. Maravelias.  
2008. Modelling fish growth: multi-model inference as a better alternative to *a priori* using von Bertalanffy equation. *Fish. Fish.* 9:178–187. [Crossref](#)
- Lane, J. Q., P. T. Raimondi, and R. M. Kudela.  
2009. Development of a logistic regression model for the prediction of toxigenic *Pseudo-nitzschia* blooms in Monterey Bay, California. *Mar. Ecol. Prog. Ser.* 383:37–51. [Crossref](#)
- Livernois, M. C., S. P. Powers, M. A. Albins, and J. F. Mareska.  
2020. Habitat associations and co-occurrence patterns of two estuarine-dependent predatory fishes. *Mar. Coast. Fish.* 12:64–77. [Crossref](#)
- Lo, N. C.-H., L. D. Jacobson, and J. L. Squire.  
1992. Indices of relative abundance from fish spotter data based on delta-lognormal models. *Can. J. Fish. Aquat. Sci.* 49:2515–2526. [Crossref](#)
- Lowerre-Barbieri, S. K., L. R. Barbieri, J. R. Flanders, A. G. Woodward, C. F. Cotton, and M. K. Knowlton.  
2008. Use of passive acoustics to determine red drum spawning in Georgia waters. *Trans. Am. Fish. Soc.* 137:562–575. [Crossref](#)
- Lowerre-Barbieri, S. K., S. L. W. Burnsed, and J. W. Bickford.  
2016. Assessing reproductive behavior important to fisheries management: a case study with red drum, *Sciaenops ocellatus*. *Ecol. Appl.* 26:979–995. [Crossref](#)
- Lowerre-Barbieri, S. K., M. D. Tringali, C. P. Shea, S. W. Burnsed, J. Bickford, M. Murphy, and C. Porch.  
2019. Assessing red drum spawning aggregations and abundance in the eastern Gulf of Mexico: a multidisciplinary approach. *ICES J. Mar. Sci.* 76:516–529. [Crossref](#)
- Lüdecke, D., M. S. Ben-Shachar, I. Patil, P. Waggoner, and D. Makowski.  
2021. performance: an R package for assessment, comparison and testing of statistical models. *J. Open Source Softw.* 6(60):3139. [Crossref](#)
- Lynch, P. D., R. D. Methot, and J. S. Link (eds.).  
2018. Implementing a next generation stock assessment enterprise: an update to the NOAA Fisheries stock assessment improvement plan. NOAA Tech. Memo. NMFS-F/SPO-183, 127 p.
- Magnuson-Stevens Fishery Conservation and Management Act, 16 U.S. Code Sect. 1801–1891d. (2020). [Available from [website](#).]
- Nelson, T. R., A. E. Jefferson, P. T. Cooper, C. A. Buckley, K. L. Heck Jr., and J. Mattila.  
2018. Eurasian perch *Perca fluviatilis* growth and fish community structure, inside and outside a marine-protected area in the Baltic Sea. *Fish. Manag. Ecol.* 25:172–185. [Crossref](#)

- Newman, D., J. Berkson, and L. Suatoni.  
2015. Current methods for setting catch limits for data-limited fish stocks in the United States. *Fish. Res.* 164:86–93. [Crossref](#)
- Ogle, D. H.  
2016. *Introductory fisheries analyses with R*, 338 p. CRC Press, Boca Raton, FL.
- Ogle, D. H., P. Wheeler, and A. Dinno.  
2021. FSA: fisheries stock analysis. R package, vers. 0.9.1. [Available from [website](#), accessed August 2021.]
- Olney, J. E., and J. M. Hoenig.  
2001. Managing a fishery under moratorium: assessment opportunities for Virginia's stocks of American shad. *Fisheries* 26(2):6–12. [Crossref](#)
- Parisien, M.-A., and M. A. Moritz.  
2009. Environmental controls on the distribution of wild-fire at multiple spatial scales. *Ecol. Monogr.* 79:127–154. [Crossref](#)
- Pauly, D.  
1980. On the interrelationships between natural mortality, growth parameters, and mean environmental temperature in 175 fish stocks. *ICES J. Mar. Sci.* 39:175–192. [Crossref](#)
- Pearson, K.  
1900. On the criterion that a given system of deviations from the probable in the case of a correlated system of variables is such that it can be reasonably supposed to have arisen from random sampling. *Lond. Edinb. Dublin Philos. Mag. J. Sci.* 50(302):157–175. [Crossref](#)
- Powers, S. P., C. L. Hightower, J. M. Drymon, and M. W. Johnson.  
2012. Age composition and distribution of red drum (*Sciaenops ocellatus*) in offshore waters of the north central Gulf of Mexico: an evaluation of a stock under a federal harvest moratorium. *Fish. Bull.* 110:283–292.
- QGIS Development Team.  
2019. QGIS Geographic Information System. Open Source Geospatial Foundation Project. [Available from [website](#), accessed July 2019.]
- R Core Team.  
2021. R: a language and environment for statistical computing. R Found. Stat. Comput., Vienna, Austria. [Available from [website](#), accessed July 2021.]
- Reyier, E. A., R. H. Lowers, D. M. Scheidt, and D. H. Adams.  
2011. Movement patterns of adult red drum, *Sciaenops ocellatus*, in shallow Florida lagoons as inferred through autonomous acoustic telemetry. *Environ. Biol. Fishes* 90:343–360. [Crossref](#)
- Rooper, J. R., G. W. Stunz, S. A. Holt, and T. J. Minello.  
2010. Population connectivity of red drum in the northern Gulf of Mexico. *Mar. Ecol. Prog. Ser.* 407:187–196. [Crossref](#)
- Sagarese, S. R., W. J. Harford, J. F. Walter, M. D. Bryan, J. J. Isely, M. W. Smith, D. R. Goethel, A. B. Rios, S. L. Cass-Calay, C. E. Porch, et al.  
2019. Lessons learned from data-limited evaluations of data-rich reef fish species in the Gulf of Mexico: implications for providing fisheries management advice for data-poor stocks. *Can. J. Fish. Aquat. Sci.* 76:1624–1639. [Crossref](#)
- SEDAR (Southeast Data, Assessment, and Review).  
2016. SEDAR 49 stock assessment report. Gulf of Mexico data-limited species: red drum, lane snapper, wenchman, yellowmouth grouper, speckled hind, snowy grouper, almaco jack, lesser amberjack, 81 p. SEDAR, North Charleston, SC. [Available from [website](#).]
- Smith, M. W., A. Y. Then, C. Wor, G. Ralph, K. H. Pollock, and J. M. Hoenig.  
2012. Recommendations for catch-curve analysis. *North Am. J. Fish. Manag.* 32:956–967. [Crossref](#)
- Then, A. Y., J. M. Hoenig, N. G. Hall, D. A. Hewitt, and E. Jardim (handling ed.).  
2015. Evaluating the predictive performance of empirical estimators of natural mortality rate using information on over 200 fish species. *ICES J. Mar. Sci.* 72:82–92. [Crossref](#)
- Tuckey, T., N. Yochum, J. Hoenig, J. Lucy, and J. Cimino.  
2007. Evaluating localized vs. large-scale management: the example of tautog in Virginia. *Fisheries* 32:21–28. [Crossref](#)
- von Bertalanffy, L.  
1938. A quantitative theory of organic growth (inquiries on growth laws. II). *Hum. Biol.* 10:181–213.
- Winner, B. L., K. E. Flaherty-Walia, T. S. Switzer, and J. L. Vecchio.  
2014. Multidecadal evidence of recovery of nearshore red drum stocks off west-central Florida and connectivity with inshore nurseries. *North Am. J. Fish. Manag.* 34:780–794. [Crossref](#)